International Journal of Mass Spectrometry 281 (2009) 15–23

Contents lists available at ScienceDirect

International Journal of Mass Spectrometry

journal homepage: www.elsevier.com/locate/ijms

Ionic diffusion and mass discrimination effects in the new generation of short flow tube SIFT-MS instruments

David Smith [a], Andriy Pysanenko [a], Patrik Španěl [a,b,*]

[a] Institute for Science and Technology in Medicine, School of Medicine, Keele University, Thornburrow Drive, Hartshill, Stoke-on-Trent ST4 7QB, UK
[b] J. Heyrovský Institute of Physical Chemistry, Academy of Sciences of the Czech Republic, Dolejškova 3, 182 23 Prague 8, Czech Republic

ARTICLE INFO

Article history:
Received 24 October 2008
Received in revised form
13 November 2008
Accepted 19 November 2008
Available online 27 November 2008

Keywords:
SIFT-MS
Ionic diffusion
Mass discrimination
Trace gas analysis

ABSTRACT

The major thrust of this paper is to describe how the current selected ion flow tube mass spectrometry (SIFT-MS) *Profile 3* instruments can be configured to provide reliable quantification of the trace gases present in air and exhaled breath by accounting for the phenomena of differential diffusion of the analytical precursor and product ions in the flow tube reactor and mass discrimination in the ion sampling/analytical quadrupole mass spectrometer/detection system. If not accounted for these phenomena, especially the latter, can result in serious errors in quantification. Hence, it is described how H_3O^+ precursor ions are totally converted to a range of product ions within the mass-to-charge ratio, m/z, range from 18 to 201 and, thus, how the ion currents collected by the downstream ion sampling orifice disc and the count rates of these ions as determined by the analytical detection system at the various m/z are used to provide values of both the diffusion enhancement coefficient, D_e, and the mass discrimination factor, M_r, that are required to allow accurate trace gas analyses. It is indicated how all such SIFT-MS instruments can be properly configured using a similar but abbreviated procedure. Finally, it is shown how the properly configured *Profile 3* instrument provides consistent and reliable analyses of acetone using H_3O^+, NO^+ and O_2^+, 2-pentanone and 2-hexanone using H_3O^+ and NO^+, and ammonia using H_3O^+ and O_2^+ precursor ions in (relatively dry) air samples and in (humid) single breath exhalations.

1. Introduction

A desired objective in selected ion flow tube mass spectrometry (SIFT-MS), towards which a considerable progress has been made over the last 10 years [1–6], is to facilitate absolute analyses of the trace gases in complex gas mixtures, including humid exhaled breath, obviating constant calibrations using gas mixtures of known trace gas concentrations. The latter are very difficult to prepare to acceptable accuracy, especially for condensable volatile organic compounds (VOCs) at low concentrations typical of those occurring in exhaled breath, which are often at the parts-per-billion (ppb) level of the matrix. Hence, SIFT-MS instruments that are properly configured together with appropriate analytical software have a major role to play in gas analysis. This has been achieved for a large laboratory SIFT instrument and the original, larger scale SIFT-MS instruments, known as TSIFT Mk.1 and Mk.2 [3,7,8], which are capable of quantifying trace gases in air and exhaled breath present at levels of about 10 ppb in a few seconds of measurement time, i.e., times typical of single breath exhalations. These instruments have been used to great effect to quantify several breath trace gases in significant populations of healthy volunteers [9,10,11]. Now it is necessary to establish a similar set-up procedure for the new generation of smaller, more sensitive commercial SIFT-MS instruments (*Profile 3*) that are beginning to be used worldwide for various applications.

We have indicated, through several publications [2,7,12], those critical SIFT-MS instrument parameters that need to be known and controlled to achieve such absolute quantifications. Ultimately, the concentration of a trace gas in the sampled air/breath introduced into the helium carrier gas in the SIFT-MS instrument flow tube (see Section 2) is derived from the ratio of the count rates of the characteristic ions formed in the reaction of the particular trace gas to that of the precursor ions (either H_3O^+, NO^+ or O_2^+ ions are used [3,8]), as determined by sampling those ions that pass through a downstream pinhole orifice and are collected into an analytical mass spectrometer/ion counting system. But this implicitly assumes that these ion count rates are themselves directly related to the product ion and precursor ion number densities in the carrier gas [12]. However, this relationship is not simple. It is influenced by (i) the differential diffusive loss rates of the product and precursor ions in the helium carrier gas/sample gas mixture that determines the currents of these ion species that reach the sampling orifice and (ii) any losses

* Corresponding author at: J. Heyrovský Institute of Physical Chemistry, Academy of Sciences of the Czech Republic, Dolejškova 3, 182 23 Prague 8, Czech Republic. Tel.: +420 2 6605 2112; fax: +420 2 8658 2307.
E-mail address: patrik.spanel@jh-inst.cas.cz (P. Španěl).

1387-3806/$ – see front matter © 2008 Elsevier B.V. All rights reserved.
doi:10.1016/j.ijms.2008.11.007

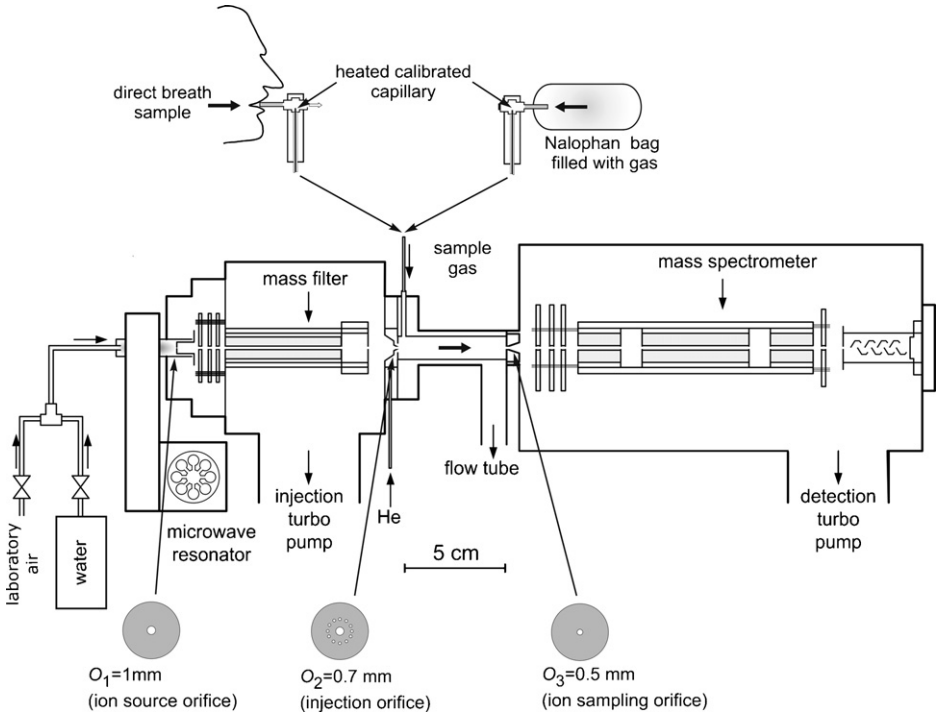

Fig. 1. Schematic diagram of the *Profile 3* SIFT-MS instrument showing the microwave discharge ion source [16], injection mass filter and the detection quadrupole mass spectrometer and the three metal discs to which ion current can be measured and which support the orifices O_1, O_2 and O_3 through which, respectively, ions pass from the ion source into the injection mass filter, mass selected ions enter the flow tube and via which ions are sampled into the analytical quadrupole mass spectrometer. Both direct breath sampling into the instrument and sampling from bag samples are illustrated.

of these ions that occur as they pass from the exit of the sampling orifice, to the entrance of the analytical (invariably a quadrupole) mass spectrometer, any discrimination to ions of different mass-to-charge ratio, m/z, in the mass spectrometer and any differences in the detection efficiency of the electron multiplier that is used to amplify individual ions to allow their count rates to be determined. The phenomena (i) and (ii) are clearly instrument-dependent in the sense that diffusive loss of ions will depend on the flow tube length, which is much shorter for the new generation of instruments than for the TSIFT instruments, and the helium/sample gas pressure and the flow speed, and discrimination in the analytical mass spectrometer/ion detection system will always be dependent on the spectrometer resolution settings and the set-up of the electron multiplier/counting system. Other parameters that are needed to realise absolute quantification of trace gases, which fortunately are easily controlled and measured accurately, include the carrier gas and sample gas flow rates and the carrier gas temperature. Also, essential parameters that are required for gas analysis by the SIFT-MS technique are the rate coefficients and the ionic products for the reactions of the chosen precursor ion species with the trace gas to be quantified at the temperature of the helium/sample gas. The details of these required conditions and the mathematics of the analyses are given in several key papers [2,3,7], that will need to be referred to again in the following sections of this paper. A recent paper presents a complete description of a numerical method that allows the calculation of absolute trace gas concentrations by SIFT-MS making no assumptions about the size and configuration of the instrument [12]. However, experimental data are essential to characterise both diffusive losses of ions in the short flow tube and mass discrimination in the particular analytical quadrupole of the *Profile 3* instruments set at particular resolutions (points (i) and (ii) above). This is the focus of the present paper.

To parameterise the influence on quantification of differential diffusion of product and precursor ions in the helium/sample gas, experiments need to be carried out in which the ion current measured to the downstream sampling orifice O_3 (see Fig. 1) is recorded as a precursor ion species at a given m/z value is totally converted to product ions at a different m/z value. This current change is a measure of the relative diffusion rates of the two ion species involved under the working conditions (flow tube length, helium/sample gas pressure and flow speed) of the particular instrument. The magnitudes of these currents are typically within the range from 10 to 200 pA which are readily measured by an in-built electrometer. To determine the *net* differential response of the ion sampling system, that is the combined effect of mass discrimination as a function of m/z of the sampled ions and the response of the ion detector (multiplier), a study of the count rate of ions, c/s, at different m/z values in relation to the ion current, i.e., the c/s per pA is required. This can be performed at any resolution setting of the analytical quadrupole mass spectrometer and the resulting data can then be programmed into the analytical software to account for these phenomena and thus allow more accurate analyses of trace gases. As mentioned above, such experimental work has been carried out previously for TSIFT Mk.1 and Mk.2 [7,8]. The present paper is concerned with the essentially similar studies that relate to the recently developed *Profile 3* SIFT-MS instruments that have much shorter flow tubes. Using this new instrument analyses of trace gases present in air and exhaled breath in the ppb and even the sub-ppb regime can be quantified to acceptable accuracy in a few seconds [13,14].

2. Specific features of the *Profile 3* SIFT-MS instrument and experimental approach

2.1. Profile 3 structure

The specific features of the first SIFT-MS instruments, the so-called TSIFT Mk.1 and Mk.2 instruments have been given in earlier publications [7,8]. They differ from the current, more sensitive, smaller *Profile 3* instruments (with which this paper is concerned) in that the flow tube in the TSIFT instruments is longer (40 cm) with

a larger diameter (4 cm). This compares with the much smaller *Profile 3* flow tube dimensions which are; length 5 cm and diameter 1 cm. In the line diagram of the *Profile 3* in Fig. 1 the mass spectrometer and flow tube elements are approximately to scale. This drive towards smaller flow tubes is motivated by the need to reduce the size of the instruments, and especially of the required pumping systems, to allow easier transportation and location in confined spaces such as surgeries and hospitals. In this regard, the weight of the *Profile 3* instrument is 120 kg compared to that of the TSIFT instruments which is typically 400 kg and the other commercially available instruments which are typically 200–500 kg [15]. However, such a drastic reduction in flow tube length has its downside in that the time available for the precursor ions to react with trace gases (see Section 1) is proportionally decreased and this implies a reduced sensitivity unless other parameters can be adjusted to compensate. In practice, this requires that the partial pressure of the sampled air in the helium carrier gas is increased and the precursor ion count rates are greater than those realised in the larger instruments. This development has required a proper investigation of the flow dynamics and improvements in the upstream precursor ion/mass spectrometer systems, but these are discussed in detail elsewhere [16]. It is sufficient to say here that through these advancements the new generation of SIFT-MS instruments are typically a factor of 10 more sensitive than the older, larger instruments, and this is allowing trace gas metabolites present in breath at the ppb level to be explored [14,17,18]. Further, it turns out that because of the radically smaller flow tube the ion diffusion losses are greatly reduced compared with the losses in the larger instruments even at the same helium carrier gas pressure and this not only boosts the precursor ion count rates (see the next section) but also simplifies the analysis. Nevertheless, these diffusion effects must be properly quantified to realise accurate analyses and this is a major focus of this paper.

2.2. SIFT-MS method and the procedure adopted for the current experiments

The SIFT-MS analytical technique has been described in detail elsewhere [2,3], but for the purposes of this paper only a brief summary is needed. SIFT-MS is distinguished from other analytical methods in that it can employ chemical ionisation using three selected reagent ions, H_3O^+, NO^+ and O_2^+, and employs fast flow tube technology coupled with accurate quantitative mass spectrometry. The chosen precursor (reagent) ion species is selected from a mixture of ion species formed in a microwave discharge through moist air by a quadrupole mass filter and injected via an orifice into fast-flowing helium carrier gas, as shown in Fig. 1. Air or breath samples containing trace gases, or indeed concentrated air/compound samples (see later), are presented to the entry port of the instrument and a sample of it enters the carrier gas at a known flow rate via a heated calibrated capillary. Characteristic product ions are produced from the reactions of each compound in the mixture with each particular precursor ion species. The choice of precursor (reagent) ion species depends on the compounds to be analysed. In the present studies we chose to use H_3O^+ ions, m/z 19, for the total conversion of this precursor ion species to ions of larger m/z in studying diffusion in the helium buffered flow tube. For a study of ammonia quantification we used both H_3O^+ and O_2^+ precursor ions. For the measurement of acetone in prepared air/acetone mixtures and in exhaled breath all three available precursor ions, H_3O^+, NO^+ and O_2^+ were used. The precursor and product ions in the carrier gas are sampled by a downstream orifice in a stainless steel sampling disc to which the total ion current is measured, labelled as O_3 in Fig. 1, and pass into the differentially pumped analytical quadrupole mass spectrometer and ion counting system. As mentioned in Section 1, it is the ratio of the count rates of the product ions to the precursor ions that is the essential parameter in the quantification of particular trace gas compounds [12]. Of great significance in the present studies is the total collection efficiency, R, describing the count rate achieved per 1 pA of ion current to the sampling disc, as will be discussed in Section 3.2.2.

There are two distinct analytical modes of operation of SIFT-MS. Firstly, the *full scan mode*, where a conventional mass spectrum is obtained over a chosen range of ion mass-to-charge ratio, m/z, principally to identify and to measure the count rates of the precursor and product ions of the analytical reactions. In the present experiments this mode was used to ensure that in the diffusion studies sufficient of a compound was added to the carrier gas to convert all the H_3O^+ precursor ions to a single product ion whence both the pA current to the sampling disc and the c/s of the precursor and product ions are be determined. For these studies we found it to be convenient to use the reactions of H_3O^+ with several ketones (acetone, 2-butanone, 2-pentanone and 2-hexanone), methanol, ethanol, benzene and toluene; the ion chemistry involved is outlined in the next section. For the exemplary breath analyses performed online in single breath exhalations, the *multiple ion monitoring mode* was used in which the downstream analytical mass spectrometer is rapidly switched between selected m/z values for both the precursor ions and the product ions, in order to quantify both water vapour [19] and the targeted trace compounds, as discussed in numerous publications (see [3]). This mode of operation provides more precise quantification of the targeted trace compounds than does the broad sweep *full scan mode*.

3. Results

The results of this study will be presented in the following order:

(1) a discussion of diffusion enhancement in the flow tube;
(2) a discussion of mass (m/z) discrimination in the ion sampling/mass spectrometer system and the derivation of the important parameter R, which is the total collection efficiency of the ions expressed in the units of c/s per pA and is a function of the m/z values of the precursor and product ions;
(3) the special case of ammonia analysis for which, uniquely, the product ions are at lower m/z values than those of the precursor ions;
(4) the formalised approach to the analysis employing the finding of (1), (2) and (3) that allows accurate quantification using particular *Profile 3* instruments;
(5) the analysis of breath ammonia and acetone using all three precursor ions as exemplars.

3.1. Diffusion in the flow tube

The precursor ions, H_3O^+, NO^+ and O_2^+, are injected into the helium carrier gas through the Venturi inlet orifice, O_2 (see Fig. 1) and are convected along the flow tube by the flowing helium carrier gas, the pressure of which is set high enough to inhibit diffusive loss of ions to the flow tube wall yet not so high that unacceptably high pressures result in the injection and detection differentially pumped mass spectrometer chambers. Thus, the chosen pressure for operation of these small instruments is close to 1 Torr of helium at which pressure it can easily be shown by experiment that the loss by diffusion of the precursor ions (m/z values 19, 30, 32) along the flow tube from the ion injector to the ion sampling is about a factor of 3. This is very much smaller than the corresponding loss in the larger, longer flow tube TSIFT instruments, which at the usual working pressure of 0.7 Torr is a factor of about 10 [7,12]. These diffusive losses are reduced somewhat when the air/breath sample gas is introduced into the helium carrier gas at a flow rate that results in a

typical partial pressure of about 0.1 Torr, because diffusion through air is much slower than through helium [20].

During SIFT-MS analyses, product ions are formed that are almost invariably of greater m/z values than those of the precursor ions (ammonia analysis being an exception; see Section 3.3) and it is generally understood that ions of larger m/z will diffuse more slowly through gases. Thus, a greater fraction of the higher m/z product ions will reach the downstream sampling orifice than are lost from the precursor ion swarm by ion-molecule reactions. This phenomenon of *diffusion enhancement* of the product ions [2,7,12] must be accounted for if accurate SIFT-MS analyses are to be performed. To quantify this phenomenon, experiments were carried out in which the change of ion current to the downstream sampling disc, pA, was measured as H_3O^+ precursor ions were totally converted to ions of greater m/z values. This was accomplished by exploiting the reactions of several ketones, M, with the H_3O^+ ions, which results in total conversion to MH^+M proton-bound dimer ions via the bimolecular and termolecular reactions sequence:

$$H_3O^+ + M \rightarrow MH^+ + H_2O; \quad MH^+ + M + He \rightarrow MH^+M + He \qquad (1)$$

Thus, for acetone with molecular weight 58 u, the final dimer ion has an m/z value of 117. Similarly, ions at m/z 145 (2-butanone), 173 (2-pentanone) and 201 (2-hexanone) were formed. Additionally, the reaction of methanol and ethanol with H_3O^+ were also exploited to form the trimer ions M_3H^+ at m/z values of 97 and 139, respectively, via reaction sequences similar to (1), and the direct proton transfer reactions of H_3O^+ with benzene and toluene to form terminating ions at m/z values of 79 and 93 according to the first reaction of sequence (1) [7]. Ion chemistry involved in the production of the $(C_2H_5OH)_3H^+$ trimer ions is discussed in a recent paper [21]. Additionally, by the addition of suitable amounts of water vapour the H_3O^+ ions can be almost totally converted to the trihydrate ion $H_3O^+(H_2O)_3$ at an m/z value of 73.

From these measurements, the ratio of the sampling disc current for a given product ion species (a particular m/z value) to the initial current of the precursor ions H_3O^+, r, was obtained in order to experimentally quantify the effect of differential diffusion for the specific operating conditions of the *Profile 3* instrument. A plot of these data is given in Fig. 2 where it can be seen that r increases as the m/z of the product ions increases, as expected due to the correlation of diffusion coefficients with the ionic mass [12,22] and reaches a value close to 2 for ions with m/z above about 100. If not accounted for, diffusion enhancement [12] would result in erroneously high values of calculated concentrations of trace gas molecules, but using the data given in Fig. 2 an accurate magnitude of the *diffusion enhancement coefficient*, D_e [12] can be used in the calculation and programmed into the SIFT-MS analytical software, as will be discussed in Section 3.4. The dashed line indicated in Fig. 2 represents the dependence of r calculated by considering differential diffusion and immediate conversion of the precursors into the products at the point of the sample inlet port according to:

$$r = \exp\left(\frac{D(H_3O^+) - D(P^+)}{\Lambda^2} t_r\right) \qquad (2)$$

Here $D(H_3O^+)$ and $D(P^+)$ are diffusion coefficients for H_3O^+ and the product ions P^+, Λ^2 is the square of the characteristic diffusion length, t_r is the reaction time. The best fit of r as a function of m/z through the experimental data points is obtained by using the previously approximated dependence of diffusion coefficient on m/z [12]:

$$D = C\frac{p_1}{p} \ln\frac{383}{m/z} \qquad (3)$$

where p_1 is a pressure of 1 Torr and p is the flow tube pressure during the measurement. The value of C is determined for the given amount of sample air in helium by the least squares method. D_e is related to r as

$$D_e = \frac{\exp((D(H_3O^+) - D(P^+))/\Lambda^2)t_r - 1}{((D(H_3O^+) - D(P^+))/\Lambda^2)t_r} = \frac{r-1}{\ln(r)} \qquad (4)$$

More details on the use of D_e in the calculation of the trace gas concentrations are given in a previous paper [12]. As a numerical example, when the current ratio for the fully converted ions $r = 2$, the corresponding diffusion enhancement coefficient for trace gas product ions is $D_e = 1.44$. In practice, a value of r for ions of chosen m/z, e.g., 201, is obtained in a simple experiment as described above and then D_e is parameterised according to Eqs. (3) and (4).

3.2. Mass discrimination in the ion sampling system

All mass spectrometer sampling/analytical systems are subject to mass (m/z) discrimination. This phenomenon is particularly sensitive to the resolution setting of the quadrupole mass spectrometer, discrimination (reduced ion current transmission) usually increasing with increase in m/z of the ion being selected. It is also influenced by the kinetic energy (velocity) of the ions in the quadrupole analytical field, i.e., the time spent by the ion in this field. But also uneven sampling of the ions in the region from their point of origin, in this case the pinhole sampling orifice, to the entrance to the quadrupole analysing field can occur and this we see in the present instrument as partial scattering of the ions in collisions with background gas (see especially Section 3.3 on ammonia analysis). Further to these factors is the possibility of a differential detection efficiency of the electron multiplier to ions of differing m/z and the energy of the ions impacting on the electron emitting surface of the multiplier. In these instruments we use an ETP multiplier, model 14553H (SGE Analytical Science Pty. Ltd.). For the present analytical work it is only required to combine these effects into a single mass discrimination factor, M_r, which is descriptive of a given instrument under the specific operating conditions, although partial delineation of the separate effects is possible, as will be shown. Note that diffusion enhancement and mass discrimination act in opposite senses, thus diminishing the overall effect, except, that is, for ammonia analysis (see Section 3.3).

To investigate the magnitudes of these discrimination effects in the *Profile 3* instrument we carried out the following experiments, which are analogous to those reported previously that relate to the larger SIFT-MS instruments [7].

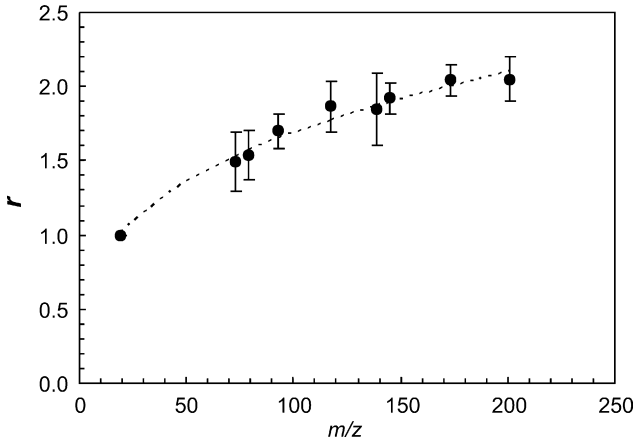

Fig. 2. The variation of r, the ratio of the current collected to the O_3 orifice disc as only H_3O^+ ions are present in the flow tube helium/sample air flowing gas ($r = 1$) to the current measured when these ions are totally converted to other ions at several m/z values, as described in Section 3.1. The error bars are estimated from the amount of conversion of the precursor ions into the terminating ions using a full kinetic model.

3.2.1. Influence of resolution of the quadrupole mass spectrometer

In all of the experiments described here the energy of the ions in the quadrupole field was set at 3 eV. Experiments were then carried out to obtain the peak structure of ions at several *m*/*z* values ranging from *m*/*z* 19 (H_3O^+) to *m*/*z* 201 (proton-bound dimer of 2-hexanone $(C_6H_{12}O)_2H^+$) for several settings of the resolution of the spectrometer. The principal reason for this was to select with confidence a resolution setting that produced acceptably narrow ion peaks that provides good separation between adjacent peaks (thus allowing quantification of the smaller peaks and hence good trace gas analysis) whilst optimising the ion current transmission of the quadrupole. A compromise between acceptable peak separation and ion transmission is an important aspect of quantitative mass spectrometry, including SIFT-MS.

To demonstrate this feature the variations of the peak width for three resolution settings of the analytical quadrupole mass spectrometer and for ions at three *m*/*z* values 19, 117 (proton-bound dimer of acetone $(C_3H_6O)_2H^+$) and 201 are shown in Fig. 3. To formalise this we indicate the peak width (in *m*/*z* value) as that at half maximum, FWHM. What is clear from these peak profiles is that both the width and height do not change greatly with changing resolution for the low *m*/*z* ions whereas they do so for the highest *m*/*z* ions when the transmission of the quadrupole mass spectrometer decreases sharply as the resolution increases. In the two organic ion peaks the ^{13}C isotopologues at *m*/*z* values one unit higher can clearly be seen showing that at the higher resolution settings good separation between adjacent *m*/*z* values is realised, but at the lower resolutions it is not. These spectra also show the well-known feature of quadrupole peaks, which is that the broadening at low resolution is biased towards lower masses and so the interference to a peak at the low *m*/*z* side of a larger peak can be severe, especially for higher *m*/*z* ions. From these observations a suitable resolution can be chosen, typically when FWHM is 0.6, which gives acceptable separation at all *m*/*z* values that allows SIFT-MS trace gas quantification to be carried out across the *m*/*z* range.

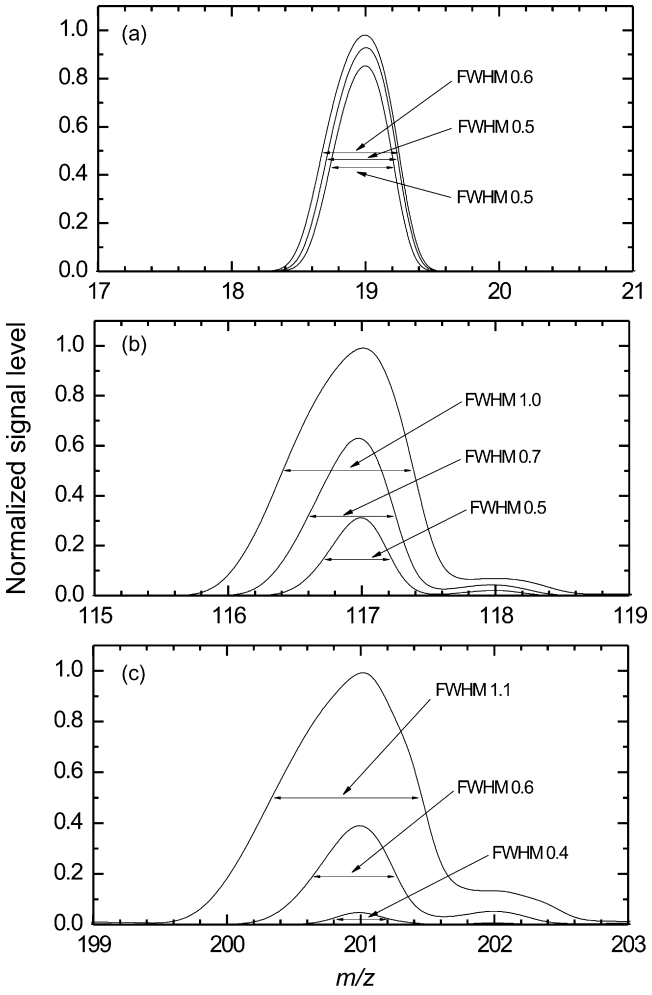

Fig. 3. Peak profiles, i.e., the signal levels against *m*/*z* for three ions at nominal values of *m*/*z* 19, 117 and 201 for three resolution settings of the analytical mass spectrometer of the *Profile 3* instrument normalized to the peak height at the lowest resolution. Note that at the highest set resolution the ^{13}C isotopologues of the two organic ions at *m*/*z* values 117 and 201 are clearly separated. The greatest spread is seen at the low *m*/*z* side of the peak, as is common for quadrupole spectrometers, and this ultimately sets the peak width requirement for quantitative analysis.

3.2.2. Determination of the total collection efficiency, R, of ions by the detection system as a function of m/z

With the quadrupole set at an acceptable resolution, measurements were made of both the ion current, pA, to the sampling disc O_3 (as shown in Fig. 1) and the count rates of the ions, c/s, for the precursor ion H_3O^+ (as injected through O_2 shown in Fig. 1) and then immediately following the total conversion of these ions to each of the several ions at different *m*/*z*, as explained in Section 3.1. This provides values of the parameter *R* in units of c/s per pA for ions at the several values of *m*/*z*. On the assumption that the fraction of the ions passing through the sampling orifice O_3 is independent of the *m*/*z* value of the ions that constitute each measured current, then *R* is a measure of the total collection efficiency of the ions as they pass from the low pressure side of O_3 to the electron multiplier via the quadrupole mass spectrometer. This same procedure can readily be performed also for the other precursor ions NO^+ and O_2^+ that are regularly used for SIFT-MS analyses. Thus, values of *R* have been obtained for ions of *m*/*z* values 19, 30, 32, 73, 79, 93, 97, 117, 139, 145, 173 and 201.

What is the significance of the values of *R*? Clearly, they provide the critical information on the transmission efficiencies of the analytical mass spectrometer system to the precursor and product ions that are required for accurate analyses. In the normal course of events in mass spectrometry, discrimination will increase with increasing *m*/*z* of the ions and hence *R* will decrease with *m*/*z* and this is the case between *m*/*z* values from 30/32 towards the value of 201, as can be seen in the inset to Fig. 4. However, unexpect-

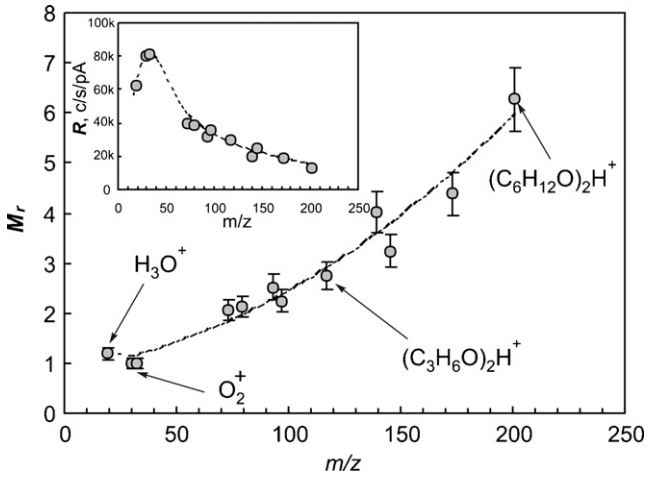

Fig. 4. The dependence of the overall mass discrimination factor, M_r, on *m*/*z* obtained by measurements for several ion species produced by the reactions of H_3O^+, as explained in Section 3.1 normalized to the O_2^+ *m*/*z* 32 value. The inset shows the measured dependence of the ratios of the count rates to the disc currents, *R* (c/s per pA), for the several values of *m*/*z*. Note the greater than unity value of M_r for H_3O^+ ions due to scattering in the analytical sampling system, as discussed in the text.

edly, the value of R for m/z 19 is consistently lower than that for m/z 30 and 32. This must indicate that these lower m/z ions are either being less efficiently collected by the mass spectrometer, i.e., some loss of H_3O^+ ions is occurring between the sampling entrance orifice and the entrance to the quadrupole, or these ions are suffering greater discrimination in the analysing field; it might be a combination of these two possible effects. We favour the first explanation that a greater scattering of the low m/z ions occurs on the background helium/air gas mixture streaming from the flow tube through the sampling orifice. Further support is given to this deduction when analysing ammonia using both H_3O^+ and O_2^+ ions, as explained in the next section. A further implication of this deduction is that the heavier ions NO^+ and O_2^+ are not scattered to such a great extent, if at all, and evidence for this is given from the analysis of acetone using all three available precursor ions, H_3O^+, NO^+ and O_2^+, as described in Section 3.5. The reduction in R for H_3O^+ ions compared with both NO^+ and O_2^+ ions is typically 20% in *Profile 3* instruments. This reduction in the collection efficiency for H_3O^+ precursor ions due to gas scattering requires a correction factor to be applied to the H_3O^+ count rate, as emphasized in Sections 3.3–3.5.

In SIFT-MS, analysis of a given trace gas compound is obtained from the *ratio* of the sum of the count rates of all the product ions formed in the reaction of the precursor ions with the compound to the count rate of the precursor ions involved in the reaction weighted by the reaction rate coefficients [12]. Now we can normalise the values of R to that for O_2^+ at an m/z value of 32 (R for NO^+ ions is not significantly different). According to the formulation used in SIFT-MS previously [7,12], we can relate R to the overall mass discrimination factor, M_r, as $R(O_2^+)/R(A^+)$ for A^+ ions at the differing m/z values. A plot of M_r against m/z is given in Fig. 4, where it can be seen, for example, that ions at m/z 201 are discriminated against in the sampling system by a factor of 6 compared to NO^+ and O_2^+ precursor ions and by a factor of 5 (i.e., 20% lower) for H_3O^+ precursor ions. Obviously, these M_r factors need to be accounted for in the analysis, as will be discussed in Section 3.4. The absence of points within the m/z region from 32 to 73 is unfortunate but unavoidable, because we have not been able to identify any ion chemistry that can produce only a single ion species from any of the three H_3O^+, NO^+ and O_2^+ precursor ions in this m/z range.

The increase of M_r with increasing m/z beyond 30/32 is entirely consistent with expectations based on general mass spectrometric considerations. The rate of increase in M_r depends on the settings of the mass spectrometer; the greater the resolution the steeper will be the increase in M_r with increasing m/z. Hence, if the conditions of the experiment are changed, such as the helium pressure, sample flow rate, analytical mass spectrometer resolution, it is necessary to perform a limited experiment along the lines of that described above to determine M_r as a function of m/z. However, in Section 3.4 we describe a simpler approach to this based on the determination of R (and hence M_r) for H_3O^+ and O_2^+ ions and the ions at m/z 117 and 201 as used in the present study.

3.3. The unique case of ammonia analysis

The ion chemistry scheme involved in the analysis of ammonia, NH_3, by SIFT-MS is unique in that the primary product ions of the reactions involved in the analysis have m/z values that are smaller than those of the precursor ions. Thus, the reaction of H_3O^+ with NH_3 results in NH_4^+ at m/z 18 and the reaction of O_2^+ with NH_3 results in NH_3^+ at m/z 17. Much SIFT-MS work has been carried out to analyse ammonia in air and especially in humid exhaled breath, initially using the larger TSIFT instruments with vacuum pumps of greater pumping speeds, and these analyses did not reveal any significantly different quantifications when using H_3O^+ and O_2^+ precursor ions [8]. However, when measuring ammonia using the *Profile 3* instrument, then it was immediately apparent that ammonia analyses, both in dry air and exhaled breath, resulted in an apparent difference in the calculated concentrations, with the ammonia as measured by O_2^+ being consistently lower than that using H_3O^+ by a factor of typically 0.65. The important clue to the reason for this unacceptable discrepancy comes from the lower collection efficiency for H_3O^+ compared to that for O_2^+, as discussed above, where this is attributed to scattering loss of low mass ions. Thus, it is logical to deduce that NH_3^+ product ions are scattered more than the O_2^+ precursor ions from which they are formed.

To investigate this discrepancy, O_2^+ precursor ions were converted totally to NH_3^+ ions by the addition of large flows of an ammonia/air mixture, as described in Section 3.2.2, and both the current to the sampling disc and the count rates of the precursor and product ions were measured before and after ammonia was introduced. Actually, the NH_3^+ product ion of the O_2^+/NH_3 reaction is rapidly converted in a secondary reaction with NH_3 to NH_4^+ in the presence of a large concentration of ammonia and so the only comparison that can be made is that of the pA for the total O_2^+ ion current and that for NH_4^+, not NH_3^+, but these ions have m/z values that differ by one m/z unit only (see the additional experiments on this described below). The results of this experiment show that the pA currents reduce by about 10% when the O_2^+ ions are totally converted to NH_4^+ ions indicating that differential diffusive loss of O_2^+ and NH_4^+ ions is small, which is consistent with the known, very similar diffusion coefficients for these ions in the helium/air mixture [22,20]. However, the c/s of the NH_4^+ ions is lower than that for the O_2^+ ions prior to their total conversion by a factor of 0.6, which is similar to the ratio given above for ammonia concentrations obtained using O_2^+ and H_3O^+ precursor ions. This surely gives support to the concept expounded above of differential scattering of the light NH_4^+ and the heavier O_2^+ ions.

To further investigate this phenomenon, a similar experiment was carried out using H_3O^+ precursor ions as they are converted totally to NH_4^+ ions. In this case the ratio of the NH_4^+ to H_3O^+ pA currents was only 0.98, which also indicates that the diffusion coefficients of these ions differ only by a very small amount, as is known [22]. However, there was a small but discernible reduction in the total c/s when changing the ions from H_3O^+ to NH_4^+, the factor being 0.95 and as such it will introduce a very small error in the analysis of ammonia using H_3O^+ precursor ions (but see below). This suggests that the lighter NH_4^+ ions are scattered to a somewhat greater degree than H_3O^+ ions. We infer, therefore, that the NH_3^+ ions will be scattered to a somewhat greater degree than NH_4^+ ions, by extrapolation by a further 5% compared to H_3O^+ ions. This small but additional amount of scattering further enhances the reduction of ammonia analysis using O_2^+ and perhaps reconciles the small difference between measured ammonia levels in air and breath (factor of 0.6) and that obtained by measuring the total conversion of O_2^+ to NH_4^+ (factor 0.65). It must be said that these straight comparisons are only feasible, because the rate coefficients for the conversion of O_2^+ to NH_3^+ and H_3O^+ to NH_4^+ are within error identical [23]. Further to this, simple measurements of the total collection efficiency R for H_3O^+ and O_2^+ which result in a ratio of 0.75, which is close to what is expected in the ratio of ammonia analyses using these two precursor ions. The actual quantification ratio of 0.65 is due to the greater degree of scattering of the lighter NH_3^+ ions. These results reconcile the O_2^+ and H_3O^+ analyses of ammonia and now this can be implemented in the SIFT-MS analytical software thus allowing both these precursor ions to be used for ammonia analysis. The success of this is shown in the results obtained for the analysis of ammonia/air mixtures and exhaled breath ammonia presented in Section 3.5 below.

3.4. Implementation of D_e and M_r into the SIFT-MS analytical software

We suggest a simple approach to the determination of both D_e and M_r for each particular SIFT-MS instrument set up based on the determination of both r and R (and hence M_r) for H_3O^+ and O_2^+ ions and the ions at m/z 117 and 201 as used in the present study (see Fig. 4). Both D_e and M_r can be then parameterised as continuous functions of m/z in the range from 32 to 201 and evaluated during analyses by the SIFT-MS analytical software, thus allowing reliable quantification of trace gases that form product ions within the range of m/z values up to 201. The approximate functional dependence of D_e on m/z in this range can be defined by a single experimentally determined parameter $r(201)$ using Eqs. (3) and (4) for interpolation:

$$D_e(m/z) = \frac{((m/z)/19)^c - 1}{\ln((m/z)/19)^c}, \quad m/z \geq 32 \tag{5}$$

Here the exponent c is calculated automatically during the software configuration as $\ln(r(201))/\ln(201/19)$. For $m/z < 32$, D_e is taken as unity, i.e., no diffusion enhancement is considered (see Fig. 2). This is also the case for the precursor ions H_3O^+ and NO^+, since their diffusion coefficients are very close to that for O_2^+ [22].

The functional dependence of M_r on m/z can be defined by a parabolic interpolation between the three experimental points M_r (32) = 1.0, M_r (117) and M_r (201) as

$$M_r(m/z) = 1 + f_{m1}(m/z - 32) + f_{m2}(m/z - 32)^2, \quad m/z \geq 32 \tag{6}$$

The coefficients f_{m1} and f_{m2} are obtained by the automated solution of a set of two linear equations (Eq. (6) evaluated for the two chosen m/z values) during the software configuration.

The M_r factors for the H_3O^+ ions relative to that for O_2^+, as determined from experimental measurements of the R values for the precursor ions, and the M_r factors for the products of ammonia represent three numerical values and thus the best approach is to simply tabulate the values of M_r at m/z 17, 18 and 19 rather than parameterise them by a continuous function in the region below m/z 32. These tabulated values can be entered during the instrument configuration and together with those parameters describing the region above m/z 32 they are stored within every data file to be used during on-line display or subsequent data analyses.

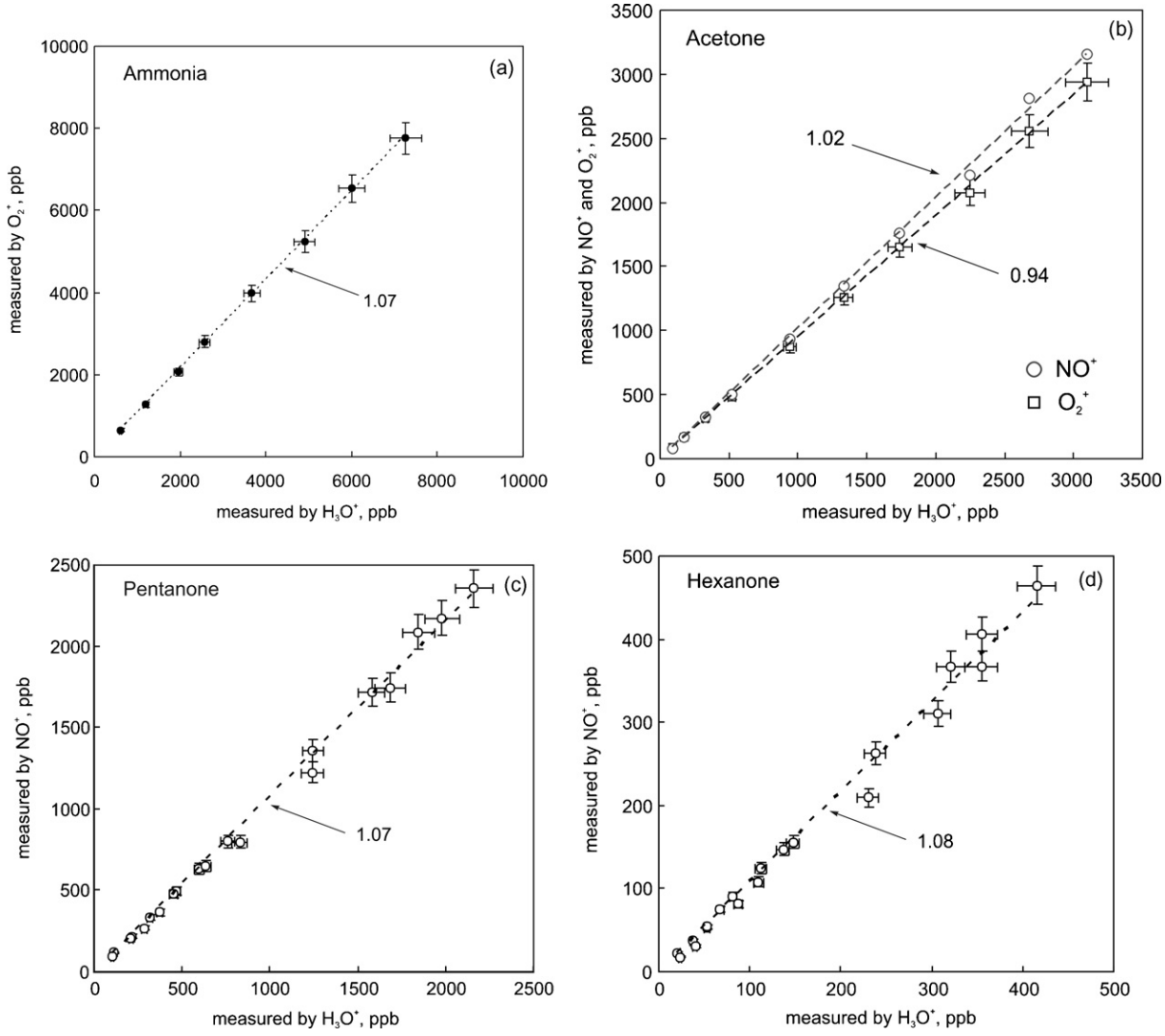

Fig. 5. (a) A plot of ammonia concentration in an air/ammonia mixture measured for O_2^+ precursor ion against that measured using H_3O^+ precursor ion. (b) Plots of the acetone concentration in air/acetone mixtures as measured using NO^+ and O_2^+ precursor ions against the concentration as measured using H_3O^+ precursor ions. (c and d) Similar plots for air/2-pentanone and air/2-hexanone mixtures as measured using NO^+ precursor ions against the concentration as measured using H_3O^+ precursor ions. The error bars represent the combined statistical errors relating to the signal levels (count rates) of both the analytical ions. These are not calibration curves but the closeness of the slopes to unity (as indicated) demonstrates the consistency of the measurements of the concentrations of these compounds using the different precursor ions.

3.5. Analysis of ammonia and acetone in air and exhaled breath

Ammonia and acetone are amongst the major metabolites in the breath of all people. This has been demonstrated by several SIFT-MS studies of the exhaled breath of cohorts of healthy individuals [11,24]. These compounds are often elevated in the breath of patients suffering from renal failure or hepatic encephalopathy [25,26]. The measurement of these compounds offers good examples of the consistency of SIFT-MS quantifications, because ammonia can be quantified using both H_3O^+ and O_2^+ and acetone can be quantified using all three precursor ions H_3O^+, NO^+ and O_2^+. Clearly, consistency in these measurements must be obtained if the instrument has been properly configured for D_e and M_r, as discussed in the previous sections of this paper. As a first check on this consistency, bag samples of both ammonia and acetone in relatively dry air were produced and analysed using the precursor ions referred to above. The results are shown in Fig. 5a and b, which are not calibration plots but simply checks on the relative analyses for the different precursor ions. As can be seen, the consistency for the analysis of ammonia using two precursor ion species (NO^+ does not react with ammonia [23]) and for acetone for the three available precursor ions are good, within ±10%, which is acceptable given the uncertainties in the D_e and M_r parameters for the precursor and product ions involved in the analytical reactions [12] and the several other parameters involved that include the reaction rate coefficients. To explore the higher m/z region of product ions, similar relative analyses were performed for the two ketones 2-pentanone and 2-hexanone and the agreement between the data obtained using H_3O^+ and NO^+ precursor ions is also within ±10%, as is seen in Fig. 5c and d.

Some years ago we carried out detailed experiments to show that the actual analyses of several trace compounds in air as performed using the larger SIFT-MS instruments (TSIFT Mk.1) were accurate to within some 10%, compounds including acetone, butanone and toluene. The measurements were carried out using the syringe injection and permeation tube techniques to generate known concentrations of compounds in flowing air samples [27,28]. These experiments demonstrated the reliability of SIFT-MS for the analysis of a wide variety of volatile organic compounds. Thus, in this paper we only show, as an example, the analysis of acetone by the *Profile 3* instrument using the three precursor ions H_3O^+, NO^+ and O_2^+.

Known concentrations of acetone in relatively dry air were prepared in the following way. A few mL of liquid acetone were introduced into a 200 mL glass bottle sealed with a septum and allowed to reach temperature equilibrium with its laboratory surrounding (typically 22C, but accurately measured). This established a known partial pressure of acetone in the headspace above its liquid, which is 26 kPa [29]. An accurate volume of this headspace is then sampled using a syringe and injected into a Nalophan bag of known volume (typically 5 L in these experiments) inflated using synthetic air. This then represents a stock acetone/air mixture, a known volume of which is sampled via a syringe (through the wall) and injected into a second bag of known volume (again about 5 L) that is connected directly to the sample inlet port of the *Profile 3* SIFT-MS instrument for analysis using H_3O^+, NO^+ and O_2^+ in sequence, measurement using each ion taking several seconds for a given concentration of acetone. The acetone level was increased incrementally by injecting further volumes of the stock acetone/air mixture into the on-line bag. Plots of the measured against expected concentration of acetone in the mixture as obtained using all three precursor ions are shown in Fig. 6. Given the simplicity of the approach to the preparation of the acetone/air mixtures and the uncertainties in other instrument parameters, as referred to in previous sections of this paper, the agreement between measured and expected acetone concentrations is good, being within 10%. Some

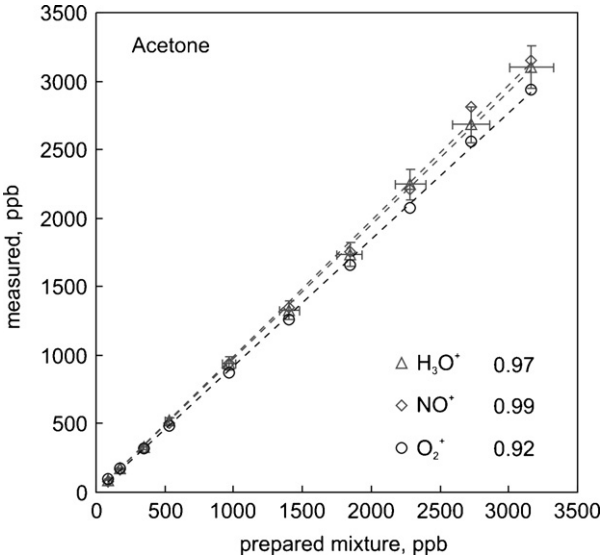

Fig. 6. Plots of the acetone concentration in air/acetone mixtures as prepared using the known vapour pressure of liquid acetone and syringe volume sampling of the liquid headspace as measured using H_3O^+, NO^+ and O_2^+ ions sequentially. These data show that acetone can be quantified to better than 10% using any of the precursor ions within the concentration range 50–3500 ppb (parts-per-billion) and given the linearity of the SIFT-MS method [14,28], reliable measurements can be made at ppb levels and below.

adsorption of acetone onto the bag surfaces might be expected, thus lowering the concentrations below that calculated from the vapour pressure and bag volumes, but clearly this is not severe for this compound, but it might well be more so for compounds with lower vapour pressures that are more condensable. Then it would presumably be necessary to heat the bags in a temperature controlled enclosure and such experiments are on going.

For the analysis of ammonia and acetone in single breath exhalations using SIFT-MS we use the multiple ion monitoring mode referred to in Section 2.2 in which the analytical mass spectrometer is switched rapidly between the precursor and product ions thus allowing analyses of single breath exhalations [3]. When using H_3O^+ precursor ions the water vapour level in the exhaled breath is also determined which represents a valuable check on other parameters involved in the analyses, especially the sample air/breath flow rate, which is known to be close to 6% by volume [19]. Sample data for the analysis of water vapour, ammonia and acetone in two sequential exhalations and inhalations from each of two male volunteers, A and B, are shown in Fig. 7. The levels of these compounds in the alveolar portion of the exhalations are indicated, water vapour in percent and the trace compounds in parts-per-billion, ppb. Also shown are the near laboratory air values obtained during the inhalations. Note the increase in the water vapour and acetone during the alveolar phases, but that this is not obvious for ammonia. This is explained by the fact that ammonia is generated largely in the oral cavity, whereas the highest levels of acetone and water vapour originate at the (somewhat higher temperature) alveolar interface. These important observations relating to oral and alveolar interface origins of trace gas compounds are reported in detail in two recent papers [30,31]. Similar measurements were made on the breath of the two volunteers using NO^+ precursor ions (for acetone only) and O_2^+ (for ammonia and acetone) and the collected results are given in Table 1. The consistency of the data for both ammonia and acetone as measured using the different precursor ions is remarkable, but quite typical of on-line SIFT-MS analyses of single breath exhalations. The consistently higher water vapour levels for volunteer B result from his somewhat higher body temperature (by about 0.5C; this is commonly observed for different

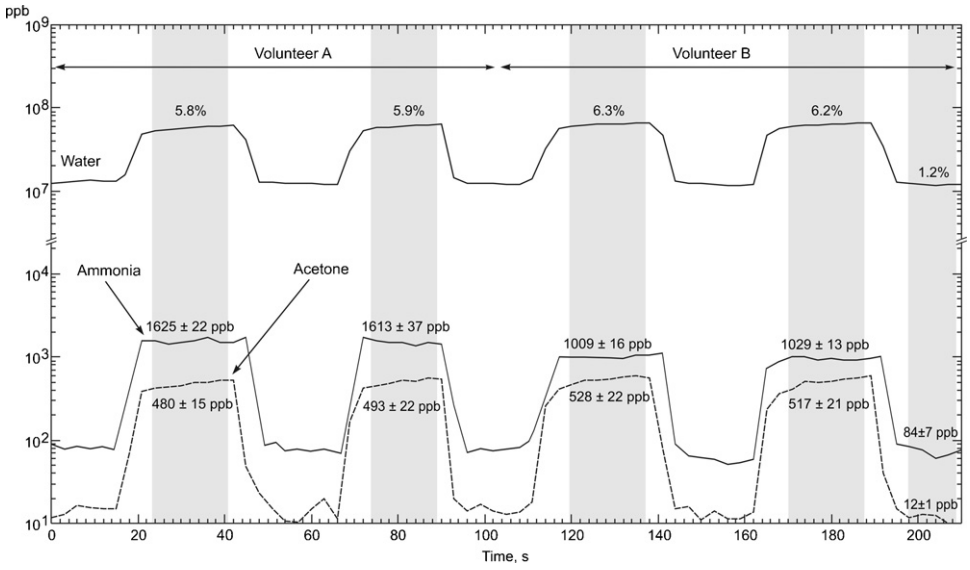

Fig. 7. Sample MIM data profiles for two sequential mouth exhalations and inhalations by two volunteers measured showing the level of water vapour (%), and acetone and ammonia (ppb). Also indicated are the levels of the compounds in the ambient laboratory air obtained during the inhalation periods shown by the shaded area to the right. Note the consistency of the levels for the two volunteers. The differing shapes of the ammonia and acetone profiles and the water vapour levels for the two volunteers are discussed in the text.

Table 1
Ammonia and acetone concentrations measured in two sequential breath exhalations (via the mouth) of two volunteers A and B obtained using the precursor ions indicated.

	Ammonia (ppb)		Acetone (ppb)	
	Exhalation 1	Exhalation 2	Exhalation 1	Exhalation 2
Volunteer A				
H_3O^+	1625 ± 22	1613 ± 37	480 ± 15	493 ± 22
NO^+			539 ± 10	510 ± 13
O_2^+	1632 ± 12	1609 ± 18	519 ± 18	557 ± 15
Volunteer B				
H_3O^+	1009 ± 17	1029 ± 14	528 ± 22	517 ± 21
NO^+			553 ± 10	531 ± 17
O_2^+	1046 ± 15	971 ± 12	537 ± 20	539 ± 20

volunteers and has been described in detail in a previous paper [32].

4. Concluding remarks

The important message of this paper is that when the current short flow tube SIFT-MS *Profile 3* instruments are properly configured for diffusion enhancement of ions in the flow tube for increasing m/z (as described by the coefficient D_e) and the collection efficiency of the ion sampling and detection system (as described by the factor M_r that is also dependent on m/z and the resolution of the quadrupole mass spectrometer) they can be used to quantify to reasonable accuracy the compounds present at trace levels in air and exhaled breath, obviating calibration for each trace gas compound. Thus, compounds with molecular weights up to about 300 u can be quantified, this upper limit being set by the maximum m/z range of the analytical quadrupole mass spectrometer. Of course, the kinetics of the reactions of the chosen precursor ion with each compound, i.e., the rate coefficient and product ions, must be known and included in the on-board kinetics library if instantaneous, on-line analyses are to be achieved. This paper describes the procedure used to set up the current *Profile 3* instruments and demonstrates the results that can be obtained via analyses of bag samples of air/ammonia/acetone and direct breath analyses.

Acknowledgement

We gratefully acknowledge partial funding from the Grant Agency of the Czech Republic (project number 202/06/0776).

References

[1] D. Smith, P. Španěl, Analyst 132 (2007) 390.
[2] P. Španěl, D. Smith, Med. Biol. Eng. Comput. 34 (1996) 409.
[3] D. Smith, P. Španěl, Mass Spectrom. Rev. 24 (2005) 661.
[4] P. Španěl, D. Smith, Eur. J. Mass Spectrom. 13 (2007) 77.
[5] P. Španěl, D. Smith in, A. Amann, D. Smith (Eds.), Breath Analysis for Clinical Diagnosis and Therapeutic Monitoring, World Scientific, Singapore, 2005, pp. 3–34.
[6] D.B. Milligan, G.J. Francis, B.J. Prince, M.J. McEwan, Anal. Chem. 79 (2007) 2537.
[7] P. Španěl, D. Smith, J. Am. Mass Spectrom. Soc. 12 (2001) 863.
[8] D. Smith, A.M. Diskin, Y. Ji, P. Španěl, Int. J. Mass Spectrom. 209 (2001) 81.
[9] A.M. Diskin, P. Španěl, D. Smith, Physiol. Meas. 24 (2003) 107.
[10] C. Turner, P. Španěl, D. Smith, Rapid Commun. Mass Spectrom. 20 (2006) 61–68. A longitudinal study of ethanol and acetaldehyde in the exhaled breath of healthy volunteers using selected-ion flow-tube mass spectrometry.
[11] C. Turner, P. Španel, D. Smith, Physiol. Meas. 27 (2006) 637.
[12] P. Španěl, K. Dryahina, D. Smith, Int. J. Mass Spectrom. 249/250 (2006) 230.
[13] B.M. Ross, N. Vermeulen, Rapid Commun. Mass Spectrom. 21 (2007) 3608.
[14] B.M. Ross, BMC Res. Notes 1 (2008) 41.
[15] G.J. Francis, P.F. Wilson, D.B. Milligan, V.S. Langford, M.J. McEwan, Int. J. Mass Spectrom. 268 (2007) 38.
[16] P. Španěl, K. Dryahina, D. Smith, Int. J. Mass Spectrom. 267 (2007) 117.
[17] P. Španěl, K. Dryahina, D. Smith, J. Breath Res. 1 (2007), 011001 (4 pp.).
[18] P. Španěl, K. Dryahina, D. Smith, J. Breath Res. 1 (2007), 026001 (8 pp.).
[19] P. Španěl, D. Smith, Rapid Commun. Mass Spectrom. 15 (2001) 563.
[20] H.W. Ellis, E.W. McDaniel, D.L. Albritton, L.A. Viehland, L. Lin, E.A. Mason, At. Data Nucl. Data Tables 22 (1978) 179–217.
[21] E. Boscaini, T. Mikoviny, A. Wisthaler, E. von Hartungen, T.D. Mark, Int. J. Mass Spectrom. 239 (2004) 215.
[22] K. Dryahina, P. Španěl, Int. J. Mass Spectrom. 244 (2005) 148.
[23] P. Španěl, D. Smith, Int. J. Mass Spectrom. 176 (1998) 203.
[24] D. Smith, C. Turner, P. Španěl, J. Breath Res. 1 (2007), 014004 (12 pp.).
[25] C. Turner, P. Španel, D. Smith, Physiol. Meas. 27 (2006) 321.
[26] S. DuBois, S. Eng, R. Bhattacharya, S. Rulyak, T. Hubbard, D. Putnam, D.J. Kearney, Dig. Dis. Sci. 50 (2005) 1780.
[27] P. Španěl, J. Cocker, B. Rajan, D. Smith, Ann. Occup. Hyg. 41 (1997) 373.
[28] D. Smith, P. Španěl, J.M. Thompson, B. Rajan, J. Cocker, P. Rolfe, Appl. Occup. Environ. Hyg. 13 (1998) 817.
[29] M. Covarrubias-Cervantes, I. Mokbel, D. Champion, J. Jose, A. Voilley, Food Chem. 85 (2004) 221.
[30] T.S. Wang, A. Pysanenko, K. Dryahina, P. Španěl, D. Smith, J. Breath Res. 2 (2008), 037013 (13 pp.).
[31] D. Smith, T.S. Wang, A. Pysanenko, P. Španěl, Rapid Commun. Mass Spectrom. 22 (2008) 783.
[32] D. Smith, T.S. Wang, P. Španěl, Physiol. Meas. 23 (2002) 477.